

## Electronic structure of hexagonal $\text{Ti}_3\text{AlC}_2$ and $\text{Ti}_3\text{AlN}_2$

Alexander L. Ivanovskii\* and Nadezhda I. Medvedeva

Institute of Solid State Chemistry, Ural Branch of the Russian Academy of Sciences, 620219 Ekaterinburg, Russian Federation.  
Fax: +7 3432 74 4495; e-mail: ivanovskii@ihim.uran.ru

The self-consistent full-potential LMTO method was used to study the electronic properties of the new hexagonal phases  $\text{Ti}_3\text{AlC}_2$  and  $\text{Ti}_3\text{AlN}_2$ , and their chemical stability was compared with the stability of the isostructural compound  $\text{Ti}_3\text{SiC}_2$  on the basis of cohesive energy calculations.

Among a large group of ternary carbides and nitrides obtained in the M-X (C,N) systems, where M is a *d* metal, and X is a group IIIB or IVB element (see ref. 1), only one phase of the composition  $\text{Ti}_3\text{SiC}_2$  was known until recently, which has a hexagonal structure (space group  $D_{6h}^4$ ,  $P6_3/mmc$ ).<sup>2–5</sup> Unusual properties of this phase (high melting temperature, chemical inertness and plasticity) made it interesting, in particular, as a candidate material for creating novel construction ceramics.<sup>6–11</sup> Nonempirical quantum-chemical calculations of  $\text{Ti}_3\text{SiC}_2$  made it possible to investigate in detail the electronic properties and chemical bonding of hexagonal titanium carbosilicide and to predict their variation for a series of hypothetical isostructural phases with different *d* metals is changed ( $\text{Zr}_3\text{SiC}_2$ ,  $\text{V}_2\text{SiC}_2$ ), when C vacancies appear (nonstoichiometry in the carbon sublattice:  $\text{Ti}_3\text{SiC}_{2-x}$ ,  $\text{V}_3\text{SiC}_{2-x}$ ) and when  $\text{Ti}_3\text{SiC}_2$ -based solid solutions are formed ( $\text{Ti}_3\text{SiC}_{2-x}\text{N}_x$ ,  $\text{Ti}_3\text{SiC}_{2-x}\text{O}_x$ ).<sup>13,14</sup>

Recently, H. D. Lee and W. T. Petuskey<sup>15</sup> found the new hexagonal phase  $\text{Ti}_3\text{AlN}_2$  in the Ti–Al–N system in a narrow temperature range (~1523–1673 K) and determined its lattice parameters. The existence of the metastable phase  $\text{Ti}_3\text{AlC}_2$ <sup>16</sup> ( $\text{Ti}_2\text{AlC}_{2-x}$ )<sup>17</sup> with a hexagonal  $\text{Ti}_3\text{SiC}_2$ -like structure was reported.

In this work we have performed self-consistent calculations of the electronic structure of the new ternary compounds  $\text{Ti}_3\text{AlC}_2$  and  $\text{Ti}_3\text{AlN}_2$  with the  $\text{Ti}_3\text{SiC}_2$ -type structure by the full-potential linear muffin-tin orbitals method (FLMTO).<sup>18</sup> The results were compared with analogous computations for isostructural titanium carbosilicide.<sup>13–15</sup>

A fragment of the crystal structure of hexagonal ( $D_{6h}^4$ )  $\text{Ti}_3\text{AlC}_2$ ,  $\text{Ti}_3\text{AlN}_2$  is given in Figure 1. The unit cell includes two formula units [6Ti, 2Al and 4(C,N) atoms]. The structure is formed by layers of adjoining octahedra  $\text{Ti}_6\text{C}$  ( $\text{Ti}_6\text{N}$ ) alternating with plane nets of Al atoms. Titanium atoms occupy two structurally nonequivalent sites [Ti(1) and Ti(2)]. Ti(1) atoms constitute the (100) layers neighbouring Al atom nets. Ti(2) atoms are located inside the carbide (nitride) layers and have carbon (nitrogen) atoms in their nearest surroundings.

Figure 2 demonstrates total and local densities of states (TDOS, LDOS) of  $\text{Ti}_3\text{AlC}_2$  and  $\text{Ti}_3\text{AlN}_2$ . The valence band of  $\text{Ti}_3\text{AlC}_2$  contains two separate energy bands (A and B, Figure 2). The lower band A is composed predominantly of C 2*s* states and is separated from the upper occupied band (B) by a forbidden gap ( $E_g$ ). The band B contains mixed contributions from Ti(1,2) 3*d*, 4*s*, 4*p*, C 2*p* and Al *s*, *p*, *d* states. The Fermi level ( $E_F$ ) is in the local TDOS minimum. The bottom of the conduction band is formed by antibonding Al 3*d*, 3*p*, Ti 3*d* and C 2*p* states.

For  $\text{Ti}_3\text{AlN}_2$ , the main changes in the TDOS are associated with an essential decrease in the energy of N 2*s* states, an increase in  $E_g$  and occupation of some antibonding (for  $\text{Ti}_3\text{AlN}_2$ ) Ti 3*d*, Al 3*d*, N 2*p* states as a result of an increase in the valence electron concentration (vec) in the cell.

The chemical stability of the hexagonal titanium alumocarbide and aluminonitride can be compared based on FLMTO calculations of their cohesive energies ( $E_{\text{coh}}$ ) determined as  $E_{\text{coh}} = E_{\text{tot}} - E_{\text{at}}$ .  $E_{\text{tot}}$  is the total energy of crystal,  $E_{\text{at}}$  is the sum of energies of isolated atoms constituting the crystal.<sup>18</sup> According to the data of Table 1, the cohesive energy of

**Table 1** Cohesive energy ( $E_{\text{coh}}$ /Ry per unit cell) and total density of states at the Fermi level [ $N(E_F)$ /Ry<sup>-1</sup>] for hexagonal ( $D_{6h}^4$ )  $\text{Ti}_3\text{AlC}_2$ ,  $\text{Ti}_3\text{AlN}_2$  as compared with  $\text{Ti}_3\text{SiC}_2$ .<sup>14</sup> FLMTO calculations.

Structure	$-E_{\text{coh}}$	$N(E_F)$	vec <sup>a</sup>
$\text{Ti}_3\text{AlC}_2$	7.223	45.66	46
$\text{Ti}_3\text{AlN}_2$	6.770	122.52	50
$\text{Ti}_3\text{SiC}_2$	7.601	75.68	48

<sup>a</sup>Valence electron concentration (e, in unit cell).

$\text{Ti}_3\text{AlC}_2$  is higher than that of  $\text{Ti}_3\text{AlN}_2$ . This fact corresponds to lowering  $E_{\text{coh}}$  in the series<sup>14</sup> of hexagonal  $\text{Ti}_3\text{AlC}_2 \rightarrow \text{Ti}_3\text{AlN}_2$ , and can be related to weakening the covalent bonds Ti(1,2)–N in comparison with Ti(1,2)–C, as it was found for ‘pure’ binary cubic (*B1*) TiC and TiN.<sup>19</sup>

Let us consider the nature of chemical bonding in  $\text{Ti}_3\text{AlC}_2$  and  $\text{Ti}_3\text{AlN}_2$  in greater detail. As follows from the present calculations, the chemical bonding in these phases is of a complex combined ionic-covalent-metallic type. The ionic component of bonding is determined by the polarization of electronic density, so that additional charges are concentrated in the muffin-tin (MT) spheres of nonmetallic atoms. The effective charges of MT spheres for  $\text{Ti}_3\text{AlC}_2$  are: Ti(1), +0.210 e; Ti(2), +0.283 e; Al, –0.219 e and C, –0.256 e. For  $\text{Ti}_3\text{AlN}_2$ , the charge polarization of Ti(2)–N increases by ~0.33 e. Also noteworthy are the differences in the charge states of structurally nonequivalent titanium atoms [Ti(1) and Ti(2)].

The metallic bonding in  $\text{Ti}_3\text{AlC}_2$ ,  $\text{Ti}_3\text{AlN}_2$  is due to the collectivisation of delocalized states. It also differs considerably for crystallographically nonequivalent atoms Ti(1) and Ti(2). This can be seen in the distribution profile of near-Fermi LDOS of Ti(1) and Ti(2) (Figure 2), which form metallic Ti–Ti bonds

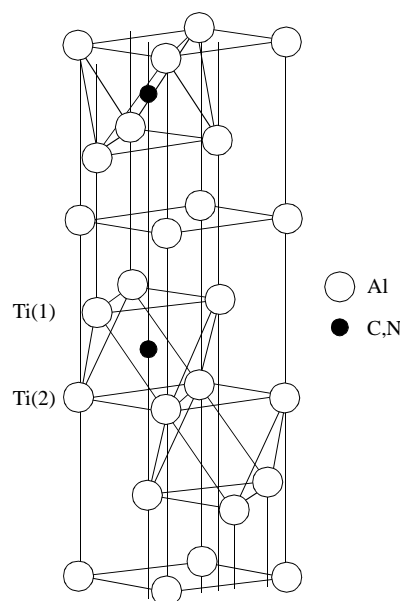


**Figure 1** Fragment of the crystal structure of hexagonal ( $D_{6h}^4$ - $P6_3/mmc$ )  $\text{Ti}_3\text{AlC}_2$ ,  $\text{Ti}_3\text{AlN}_2$ .

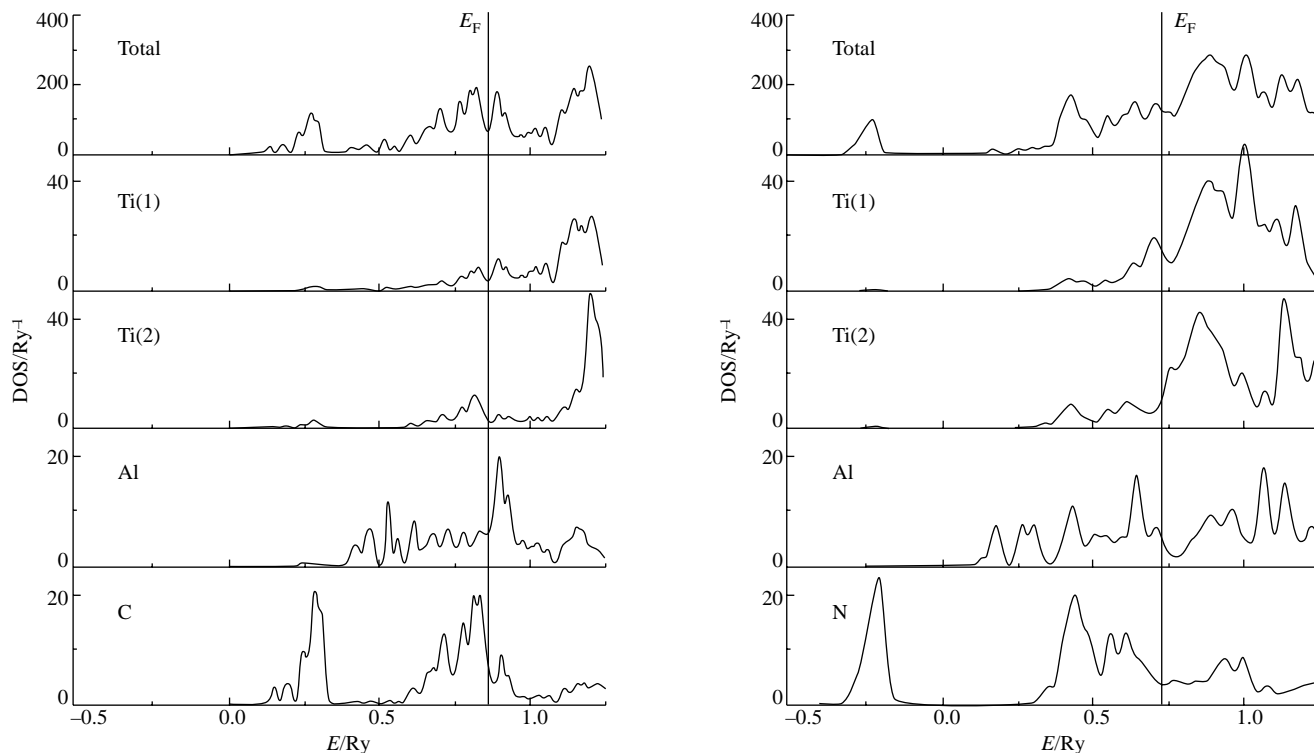


Figure 2 Total DOS (top) and local DOS of  $\text{Ti}_3\text{AlC}_2$  and  $\text{Ti}_3\text{AlN}_2$ .

in the crystal. The ratio of LDOS at the Fermi level [ $N(E_F)$ ] for nonequivalent centres [ $N(E_F)^{\text{Ti}(1)}/N(E_F)^{\text{Ti}(2)}$ ], which is 1.91 for  $\text{Ti}_3\text{AlC}_2$ , can serve as a qualitative characteristic of the degree of anisotropy of metallic bonds. Note that, in spite of the rapid growth of the total  $N(E_F)$  for  $\text{Ti}_3\text{AlN}_3$  (Table 1), *i.e.* 'metallisation' of the aluminonitride, the ratio [ $N(E_F)^{\text{Ti}(1)}/N(E_F)^{\text{Ti}(2)}$ ] changes rather insignificantly ( $\sim 1.83$ ).

The above anisotropy of separate [Ti(1)–Ti(1) and Ti(2)–Ti(2)] bonds can be clearly seen in Figure 3 where the maps of valence charge densities (CD) in the (100) planes including Ti(1) and Ti(2) atoms are presented. Ti(2) atoms have the maximum number of carbon atoms in their nearest surroundings and form the strongest covalent bonds Ti(2)–C. As a result, Ti(2)–Ti(2) bonds are relatively small, whereas for Ti(1) atoms (at the boundary with plane nets of Al atoms) the CD concentration in the interatomic space [Ti(1)–Ti(1) bond] is much more considerable (Figure 3).

Taking into account the layered structure of the hexagonal phases, a formal analogy can be drawn between the evolution of separate types of bonds (covalent and metallic) for nonequivalent titanium atoms, for example, in  $\text{Ti}_3\text{AlC}_2$  and in the proximity of the polar (111) face of cubic TiC (see ref. 20). In both cases, the weakening of the covalent bond Ti–C [for Ti(1) atoms of the alumocarbide or Ti atoms of the outer monolayer of the (111) face of TiC] considerably strengthens the metallicity of the bond as a consequence of redistribution of electrons between the subbands of Ti 3*d*-C 2*p* (*p*-*d* covalent bond) and Ti 3*d*, 4*s* (*d*-*d* metallic bond) states.

The 'layered' anisotropy of covalent bonds can be seen in Figure 2. For  $\text{Ti}_3\text{AlC}_2$ , the LDOS maximum of Ti(2) coincides with LDOS maxima of carbon atoms. This fact is indicative of the formation of local hybrid bonds Ti(2)–C inside the 'carbide' layer, as it takes place in binary cubic carbides.<sup>19</sup> The LDOS of Ti(1) has a more complicated shape and reflects both the

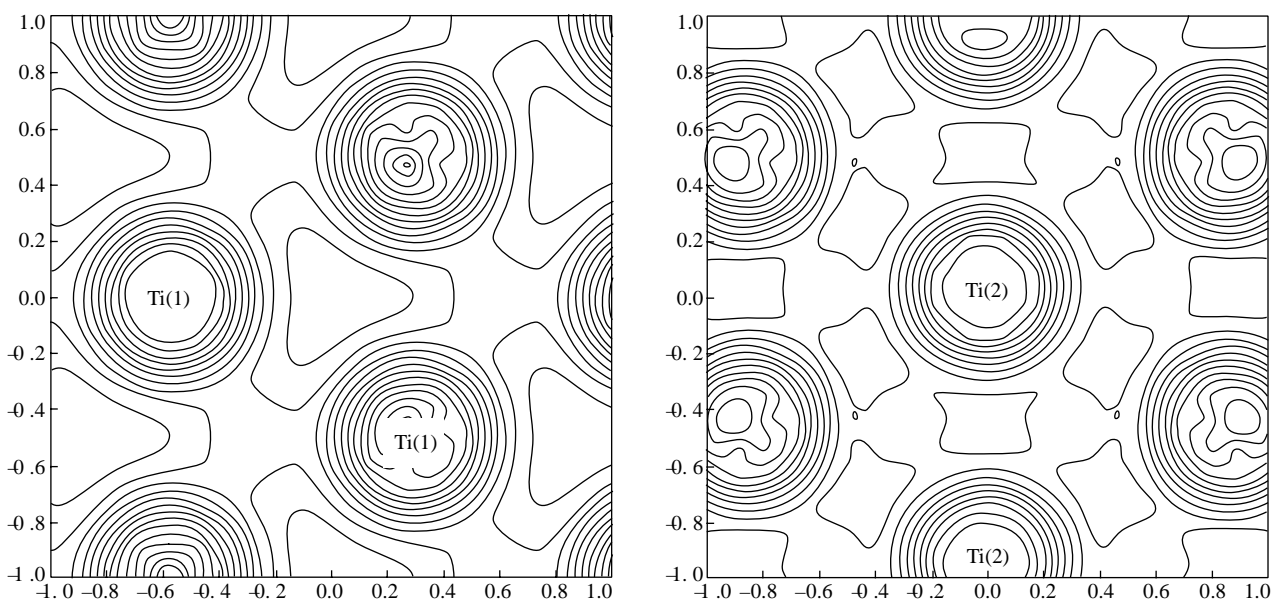


Figure 3 Charge density distribution in the (100) monolayers composed of Ti(1) and Ti(2) atoms (see Figure 1) for  $\text{Ti}_3\text{AlC}_2$  according to FLMTO calculations.

formation of the covalent bonds Ti(1)-C inside the octahedra and the 'interlayer' interaction Ti(1)-Al. As follows from the analysis performed, the covalent bonds C-Ti(1)-Al (along the *c* axis, Figure 1) are considerably weaker than the C-Ti(2)-C bonds. Note that, in the organization of Ti-Al and Al-Al hybrid bonds, 3*d* functions of aluminium, which are vacant in the atomic state, take part. Thus, according to our calculations, the electronic configuration of aluminium in Ti<sub>3</sub>AlC<sub>2</sub> is Al 3s<sup>1.203</sup> 3p<sup>1.703</sup> 3d<sup>0.313</sup>.

Until the present time, the physico-chemical properties of Ti<sub>3</sub>AlC<sub>2</sub> and Ti<sub>3</sub>AlN<sub>2</sub> have not been studied. Based on the computations, the following tentative predictions can be made.

The properties of the hexagonal alumocarbide determined by the cohesive energy (for example, thermomechanical properties such as hardness, thermal stability, enthalpy of formation, etc.), and the chemical stability will be better than those for the isostructural titanium aluminonitride. At the same time, the cohesive properties of these phases will be inferior to those of Ti<sub>3</sub>SiC<sub>2</sub>.

The metallic properties determined by the concentration of delocalised states will be anisotropic and much higher for Ti<sub>3</sub>AlN<sub>2</sub> than for Ti<sub>3</sub>AlC<sub>2</sub>.

For Ti<sub>3</sub>AlC<sub>2</sub>,  $E_F$  is in the local TDOS minimum, and  $E_F$  for Ti<sub>3</sub>AlN<sub>2</sub> is located on a plateau in the vicinity of the local TDOS maximum (Figure 2). Consequently, the change of  $v_{ec}$  in the Ti<sub>3</sub>AlN<sub>2</sub> cell (for instance, owing to the formation of lattice vacancies or the presence of substitutional impurities) does not lead to abrupt changes in  $N(E_F)$  and in the total energy of the crystal, as is the case for Ti<sub>3</sub>AlC<sub>2</sub>. Hence, based on the known chemical stability–electronic structure relationship,<sup>21,22</sup> it should be expected that nonstoichiometric phases like substitutional solid solutions will form more probably on the basis of Ti<sub>3</sub>AlN<sub>2</sub> than on the basis of Ti<sub>3</sub>AlC<sub>2</sub>.

This work was supported by the Russian Foundation for Basic Research (grant no. 96-03-32037).

## References

1 A. L. Ivanovskii, A. I. Gusev and G. P. Shveikin, *Kvantovaya khimiya v materialovedenii. Troinye karbidy i nitridy perekhodnykh metallov i elementov IIIb, IVb podgrupp (Quantum Chemistry in Materials Science. Ternary Carbides and Nitrides Based on Transition Metals and IIIb, IVb Subgroup Elements)*, Nauka, Ekaterinburg, 1996 (in Russian).

2 W. Jeitschko and H. Nowotny, *Monatsh. Chem.*, 1967, **98**, 329.  
 3 J. Nickl, K. K. Schweitzler and P. Luxenburg, *J. Less-Common Met.*, 1972, **26**, 335.  
 4 B. Gottselig, E. Gyarmati, A. Naoumidis and H. Nickel, *J. Eur. Ceram. Soc.*, 1990, **6**, 153.  
 5 T. Goto and T. Hirai, *Mater. Res. Bull.*, 1987, **22**, 1195.  
 6 J. Lis, R. Pampuch, J. Piekarczyk and L. Stobierski, *Ceram. Ont.*, 1993, **19**, 219.  
 7 R. Pampuch, J. Lis, J. Piekarczyk and L. Stobierski, *J. Mater. Synth. Proc.*, 1993, **1**, 93.  
 8 C. Recault, F. Langlais and C. Bernard, *J. Mater. Sci.*, 1994, **29**, 3941.  
 9 C. Recault, F. Langlais, R. Naslain and Y. Kihn, *J. Mater. Sci.*, 1994, **29**, 5023.  
 10 P. Komarenko and D. E. Clarc, *Ceram. Eng. Sci. Proc.*, 1994, **15**, 1028.  
 11 B. Goldin, P. V. Istomin and Yu. I. Rjabkov, *Neorg. Mater.*, 1997, **33**, 691 [*Inorg. Mater. (Engl. Transl.)*, 1997, **33**, 577].  
 12 A. L. Ivanovskii, D. L. Novikov and G. P. Shveikin, *Mendelev Comm.*, 1995, 90.  
 13 N. I. Medvedeva and A. L. Ivanovskii, *Zh. Neorg. Khim.*, 1998, **43**, 336 (*Russ. J. Inorg. Chem.*, 1998, **43**, 398).  
 14 N. I. Medvedeva, A. L. Ivanovskii, G. P. Shveikin, D. L. Novikov and D. J. Freeman, *Phys. Rev. B*, 1998, **54**, 16042.  
 15 H. D. Lee and W. T. Petuskey, *J. Am. Ceram. Soc.*, 1997, **80**, 604.  
 16 M. A. Pietzka and J. C. Schuster, *J. Phase Equilib.*, 1994, **15**, 392.  
 17 M. A. Pietzka and J. C. Schuster, *J. Am. Ceram. Soc.*, 1996, **79**, 2321.  
 18 M. Methfessel and H. Scheffer, *Physica*, 1991, **B172**, 175.  
 19 A. L. Ivanovskii and G. P. Shveikin, *Phys. Status Solidi B*, 1994, **181**, 251.  
 20 A. L. Ivanovskii and V. A. Zhilyaev, *Phys. Status Solidi B*, 1991, **168**, 9.  
 21 J. Xu and A. J. Freeman, *Phys. Rev. B*, 1989, **40**, 11927.  
 22 X. Wang, D.-C. Tian and L. Wang, *J. Phys.: Condens. Matter*, 1994, **6**, 10185.

Received: Moscow, 17th August 1998

Cambridge, 17th November 1998; Com. 8/06561F